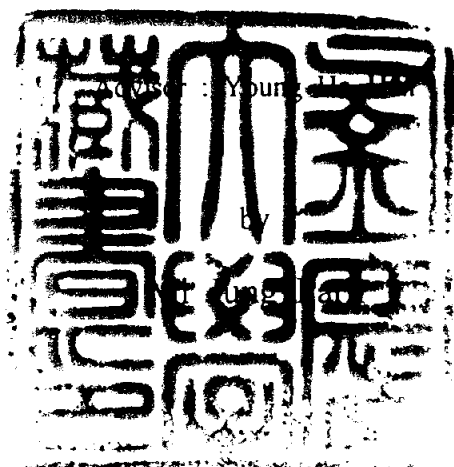


Characteristics of Heat Flux and Turbulent  
Kinetic Energy over the Yellow Sea and the  
South Sea

황해와 남해의 열속과 난류운동에너지 특성



A thesis submitted in partial fulfillment of the requirements  
for the degree of

Master of Science

in the Department of Environmental Atmospheric Sciences, Graduate School,  
Pukyong National University

February 2003


Characteristics of Heat Flux and Turbulent Kinetic Energy  
over the Yellow Sea and the South Sea

A Dissertation

by

Mi Jung Park

Approved as to style and content by :

  
\_\_\_\_\_

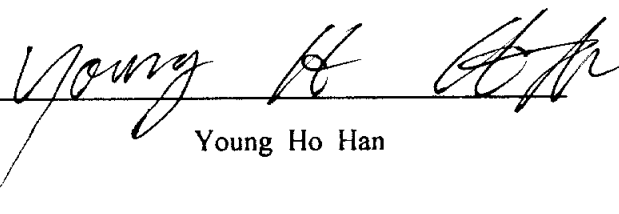
(Chairman)

Young-Seup Kim

  
\_\_\_\_\_

(Member)

Byung-Hyuk Kwon

  
\_\_\_\_\_

(Member)

Young Ho Han

December 26, 2002

# Contents

List of Figures .....	ii
List of Tables .....	iv
Abstract .....	1
1. Introduction .....	3
2. Data and methods .....	7
2.1 Buoy data .....	7
2.2 Heat balance .....	11
2.3 Turbulent kinetic energy and stability .....	15
3. Variations of the sea surface heat fluxes .....	20
3.1 Monthly and annual means .....	20
3.2 Diurnal means during winter season .....	27
4. Heat fluxes during the cold air outbreak .....	34
5. Turbulent kinetic energy (TKE) .....	39
6. Conclusions .....	46
Reference .....	48
Acknowledgments .....	53

## List of Figures

Fig. 1. Map of the adjacent seas of Korea Peninsula showing the location of ocean buoys. ....	10
Fig. 2. The seasonal variation of the monthly mean fluxes over the Yellow Sea (#22101, #22102) and the South Sea (#22103, #22104) from 1996 to 2002. ....	23
Fig. 3. The seasonal variation of the monthly mean wind speed (WS), the difference of sea-air temperature (DT), the difference of sea-air specific humidity (DQ) over the Yellow Sea (#22101) and the South Sea (#22103) for the same period as Fig. 2. ....	25
Fig. 4. The seasonal variation of the monthly mean spatial difference between the Yellow Sea (#22101) and the South Sea (#22103). ....	26
Fig. 5. Time series of the air pressure (P), wind speed (WS), air temperature (AT), and sea surface temperature (SST) over the Yellow Sea and the South Sea from December 2001 to February 2002. ....	29
Fig. 6. Monthly wind roses over the Yellow Sea (left) and the South Sea (right) for the same period as Fig. 5. ....	31
Fig. 7. Time series of the total surface heat flux over (a) the Yellow Sea and (b) the South Sea for the same period as Fig. 5. ....	32
Fig. 8. Time series of the sensible heat ( $Q_H$ ) and latent heat ( $Q_E$ ) fluxes over (a) the Yellow Sea and (b) the South Sea for the	

same period as Fig. 5. ....	33
Fig. 9. Synoptic surface weather maps associated with the cold air outbreak from the 21st to 24th of January, 2002. ....	36
Fig. 10. Time series of the sensible heat ( $Q_H$ ) and latent heat ( $Q_E$ ) fluxes over (a) the Yellow Sea and (b) South Sea for the same period as Fig. 9. ....	37
Fig. 11. Time series of the wind speed (WS), the difference of the sea-air temperature (DT), and the difference of sea-air specific humidity (DQ) over the Yellow Sea and the South Sea for the same period as Fig. 9. ....	38
Fig. 12. Dynamic production term and thermal production term over the Yellow Sea (#22101) and the South Sea (#22103) from December 2001 to February 2002. ....	42
Fig. 13. Variation of the stability parameters ( $z/L$ and $\sigma/L$ ) over the Yellow Sea (#22101) and the South Sea (#22103) for the same period as Fig. 12. ....	43
Fig. 14. Dependence of the friction velocity ( $u_*$ ) on the stability parameter $z/L$ during the cold air outbreak and winter season over (a) the Yellow Sea and (b) the South Sea. ....	44
Fig. 15. Dependence of the latent heat flux ( $Q_E$ ) on the stability parameter $z/L$ over (a) the Yellow Sea and (b) the South Sea for the same period as Fig. 14. ....	45

## **List of Tables**

Table 1. Locations of buoys and periods for this study. ....	9
Table 2. Parameters in expressions for neutral bulk transfer coefficients. ....	14
Table 3. Values of the variables and constants in (2)~(5): $I_0$ is referred to in Seckel and Beaudry (1973), Reed (1977). ....	14

# **Characteristics of Heat Flux and Turbulent Kinetic Energy over the Yellow Sea and the South Sea**

Mi Jung Park

*Department of Environmental Atmospheric Sciences, Graduate School,  
Pukyong National University*

## **Abstract**

Heat exchange between the atmosphere and the sea is analyzed using the data obtained from 3 m discus buoy installed and operated by Korea Meteorological Administration (KMA) from July 1996. The meteorological and oceanic characteristics at four buoys over the Yellow Sea and the South Sea for the period July 1996~May 2002 are discussed. The heat fluxes at each site are estimated from bulk aerodynamic method. Variation of the total heat flux considerably influenced by the latent heat flux in autumn and winter is larger over the South Sea than over the Yellow Sea. Especially, the heat loss by the sensible heat and latent heat fluxes increases gradually over the Yellow Sea and the South Sea during the cold air outbreak. The sensible heat flux is accounted for intensity of wind and the difference

of sea-air specific humidity over the South Sea. In the analysis of turbulent kinetic energy, the dynamic energy production is dominant over the South Sea than over the Yellow Sea, and the thermal energy production is comparable at the both sides. The stability of the surface layer depends on the wind speed during the winter season. The stability parameter ( $z/L$  or  $\sigma/L$ ) varies little over the South Sea, which implies that the marine atmospheric surface layer is well conserved.



## 1. Introduction

The air-sea interaction represents the study of processes which influence the transport of momentum, heat, moisture across the air-sea interface. Such processes include, for example, the pressure forcing of surface waves, dissipation of surface waves via breaking, energy flux within the wave spectrum, evaporation, bubble bursting, buoyant fluxes, turbulent transport, diffusion in the highly inhomogeneous laminar sublayers (with and without films), and transport via organized motions within the adjacent boundary layers (Geernaert, 1999). In the study of marine atmospheric boundary layer (MABL), The depth of MABL is a key to the understanding and prediction of other processes taking place within the MABL. Surface flux parameters and background atmospheric conditions bring more insight into the variability of MABL height (Joffre *et al.*, 2001).

The sensible and latent heat supplied to the atmosphere from the ocean appeared far greater than the energy conversion to kinetic energy of disturbances, and that most of the energy transferred through the interface should provide an input into the reservoir of the total potential energy of the atmosphere (Agee and Howley, 1977). Calculation of the heat flux across the ocean surface requires the combination of estimates of the component contributions. These are poorly known, due to both the paucity of data and the uncertainties of formulas governing the heat

transfers. Over the majority of the ocean surface the dominant contributions to the surface balance arise from the solar radiations, the estimation of which requires knowledge of the distribution and properties of cloud, and latent heat flux, calculation of which is reliant on the bulk formulae and dependent upon the winds, stability and gradient of humidity in the atmosphere (Schlesinger, 1990).

The Kuroshio and the Asian Monsoon are two important factors that characterize the climate of the Yellow Sea and the South Sea. The Kuroshio splits into two branches at the southwest of Kyushu, and the main branch flows along the Pacific coast of the Japan Islands toward east, and the other, named the Tsushima Warm Current, penetrates into the South Sea. The heat transport by these warm currents play an important role in the heat budget in the two marginal seas (Kondo, 1985; Lie and Cho, 1994; Ichikawa and Beardsley, 2002). The typical pattern of the Monsoon is created by the seasonal variation of polar continental air mass and the tropical maritime air mass. During the winter-monsoon season from November to March, a strong northerly winter-monsoon advects cold and dry air mass southward. In this way, the Kuroshio and the winter Monsoon over these marginal seas produce large gradients of temperature and humidity between the air and sea, which causes substantial heat exchange across the sea surface (Kim and Kimura, 1999).

A large amount of heat and moisture is supplied from the sea

surface to the atmosphere and the cold air mass is extremely modified over the warm oceanic regions such as the Kuroshio and the Gulf Stream during the winter seasons. Manabe (1957; 1958) and Ninomiya (1968) estimated the heat and moisture supplied from the sea surface over the East Sea area and they found that the sensible heat and latent heat fluxes during the cold air outbreak as about  $700 \text{ W m}^{-2}$ . Furthermore, most of the studies on the heat budget is limited to the East/Japan Sea area (Miyazaki, 1952; MMO, 1972; Kondo, 1976; Shim and Kim, 1981; Kato and Asai, 1983; Kim, 1992; Kang *et al.*, 1994; Kim and Kang, 1995; Park *et al.*, 1995; Hirose *et al.*, 1996). Several studies have been reported on the surface heat fluxes all over the East China Sea and the Yellow Sea based on the bulk method using a large amount of data (Ishii and Kondo, 1987; Sakurai *et al.*, 1989; Kim, 1992; Kang *et al.*, 1994; Hirose, 1995; Hirose *et al.*, 1999; Kim and Kimura, 1999). In the Yellow Sea, Han and Chang (1978) computed the sum of sensible heat and latent heat fluxes in winter with the budget method with a result of about  $315 \text{ W m}^{-2}$ . Recently, the maximum outflux of sensible heat from the sea surface occurred in January and the maximum influx in July (Youn *et al.*, 1998). The outgoing latent heat flux showed the maximum values in autumn. The net latent heat loss from the sea is larger than the net sensible heat loss except in January and February (Kang *et al.*, 2001).

Heat exchange between the atmosphere and the near sea around the

Korea Peninsular is produced from 3m discus buoys installed and operated by Korea Meteorological Administration (KMA) from July 1996. Instrumented ocean buoys provide an additional means of obtaining weather data at the sea. They have provided regularly data every hours. Thus, they may be most suitable means to investigate the features of cyclones or storms passing them, and to estimate heat fluxes, especially during the cold air outbreak and so on.

In the present study, each component of the heat fluxes at the sea surface is estimated by using the bulk aerodynamic formulas, based on the hourly ocean buoy data obtained regularly over the Yellow Sea and the South Sea from July 1996 to May 2002. The mechanism of heat fluxes (sensible heat and latent heat fluxes) development is analyzed from the viewpoint of a turbulent kinetic energy. The stability of the atmospheric surface layer over the sea and more detailed features in winter and the cold air outbreak when the heat exchange between the air-sea takes place actively, are presented.

## **2. Data and methods**

### **2.1 Buoy data**

Ocean weather buoys that monitors weather condition or environment change over ocean are divided into moored buoy and drifting buoy. Moored buoys are the weather sentinels of the sea. They are deployed in the coastal and offshore waters. Moored buoys measure and transmit barometric pressure, wind direction, speed and gust, air and sea temperature, and wave energy spectra from which significant wave height, dominant wave period, and average wave period are derived. Even the direction of wave propagation is measured on many moored buoys. As years go by, moored buoys play an important role in production of fundamental data that have need of weather forecast on the ocean.

Moored buoys includes the different types of buoy hulls: 3 m, 10 m, 12 m discus hulls, and 6 m boat shaped (NOMAD) hulls. In this study, we used data from 3 m discus buoy operated by KMA from July 1996. The aluminum-hulled, 3 m discus is very coast-effective but does not offer long-term survivability that the larger discus hulls provide. The transportability of the 3 m buoy is much improved over that of the larger discus buoys. It can be easily carried on a flat-bed trailer. Since it is constructed of aluminum, it is less likely to corrode, and compass

measurements are not affected.

The buoy's onboard sensors measured mean wind speed and direction at both 3.8 m and 4.8 m above sea surface and air temperature and relative humidity at 3.5 m. Sea surface temperature sensor is located at a depth of 1 m, and barometer is located inside the hull at the sea level. The measured data are to be transmitted to land by real time.

Positions and Periods of five buoys installed in the adjacent seas of Korea peninsular are shown in Table 1: international buoy #22101 (Dukjukdo), #22102 (Chilbaldo), #22103 (Geomundo), #22104 (Geojado), #22105 (the East Sea). Four of them are used in this study: two buoys are located in the Yellow Sea (#22101, #22102), the other buoys are located in the South Sea (#22103, #22104). Fig. 1 shows the locations of the four buoys currently sited in the Yellow Sea and the South Sea. The data of twelve variables have been taken regularly every hours. Five meteorological parameters (wind speed, wind direction, air pressure, air temperature and sea surface temperature) are used for calculating the heat exchange between the air-sea. The humidity parameter from the buoy was not used since in part to the difficulty in obtaining reliable measurements of boundary layer moisture from unattended instruments over open ocean for extended time periods (Breaker *et al.*, 1998). It is necessary to point out that buoy data in this study are preprocessed as follows: when the buoy is not in good condition according to observational reports, the data can not be used. The daily heat fluxes

were calculated by using the bulk aerodynamic formulas from the daily-averaged variables.

**Table 1.** Locations of buoys and periods for this study.

Buoys	Positions	Periods
#22101	37° 14' N, 126° 01' E	July 1996 ~ May 2002
#22102	34° 48' N, 125° 47' E	July 1996 ~ May 2002
#22103	34° 00' N, 127° 30' E	January 1998 ~ May 2002
#22104	34° 46' N, 128° 54' E	June 1999 ~ May 2002
#22105	37° 32' N, 129° 12' E	May 2001 ~ May 2002

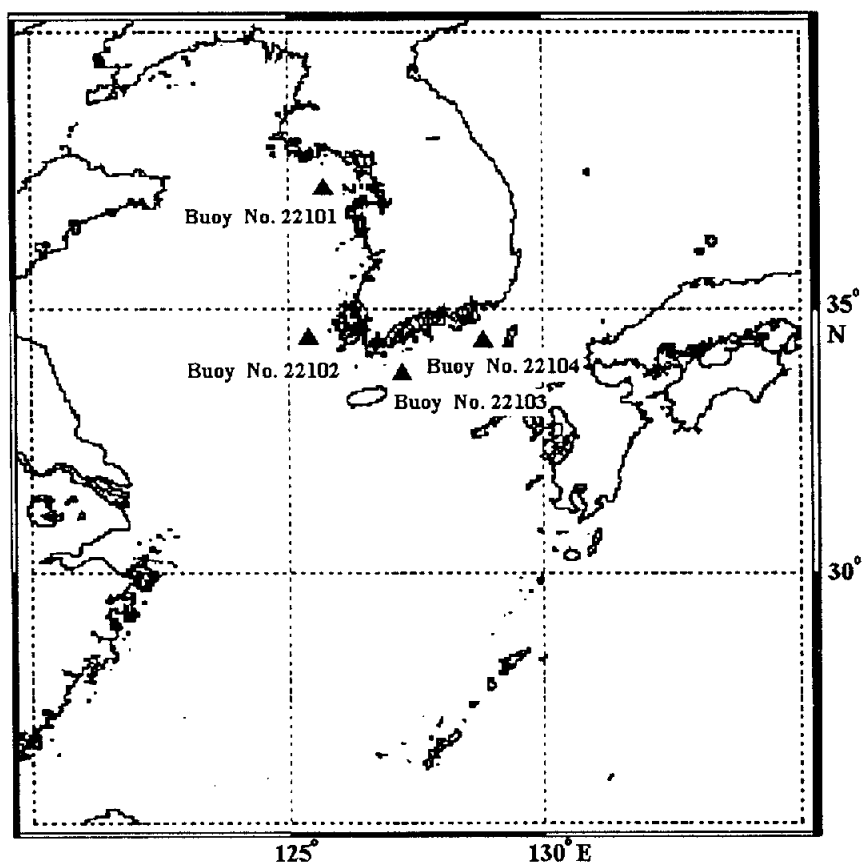


**Fig. 1.** Map of the adjacent seas of Korea Peninsula showing the location of ocean buoys.



## 2.2 Heat balance

Without a bottom boundary on the atmosphere there would be no boundary layer. Friction at the surface slows the wind, and heat and moisture fluxes from the surface modify the state of the boundary layer. The heat and moisture fluxes are driven, in turn, by the external forcings such as radiation from the sun or transpiration from plants. Forcings across the top of the boundary layer also alter mean characteristics within it.

Turbulence by itself cannot transfer heat, momentum, or moisture across the interface from the ocean or from the earth. Even ocean waves and turbulence have little direct coupling to atmospheric turbulence. Once in the air, turbulence takes over to transport momentum, heat and other constituents to greater depths in the atmosphere. The molecular and turbulent transport processes work together.

To simplify equations for the surface layer evolution, it is convenient to define an effective turbulent flux that is the sum of the molecular and turbulent fluxes. At the surface where there is no turbulent flux, the effective surface turbulent flux has a magnitude equal to that of the molecular flux. Above the lowest few centimeters, however the molecular contribution is so small that it can be neglected compared to the turbulent flux.

The net (or total) heat flux through the sea surface  $Q_T$  can be

expressed as

$$Q_T = Q_S - Q_B - Q_H - Q_E \quad (1)$$

where  $Q_S$  and  $Q_B$  are the short- and longwave radiation fluxes and  $Q_H$  and  $Q_E$  are the sensible heat and latent heat fluxes, respectively. Each component of the heat fluxes is calculated by the empirical formulas:

$$Q_S = 0.865 I_0 (1 - \alpha), \quad (2)$$

$$Q_B = \varepsilon \sigma T_a^4 (0.254 - 0.00495 e_a) + 4 \varepsilon \sigma T_a^3 (T_s - T_a), \quad (3)$$

$$Q_H = \rho_a C_p C_H (T_s - T_a) U, \quad (4)$$

$$Q_E = \rho_a L C_E (q_s - q_a) U. \quad (5)$$

Equations (2) and (3) were proposed by Kim and Kimura (1995) and Efimova (1961) with the amount of cloud, respectively. The bulk transfer coefficients ( $C_H$  and  $C_E$ ) of Kondo (1975) are adopted for equations (4), (5). When the wind speed is expressed in units of  $\text{m s}^{-1}$ , the formulae are given by

$$10^3 C_H(10 \text{ m}) = a_h + b_h u_{10}^{p_h} + c_h (u_{10} - 8)^2 \quad (6)$$

$$10^3 C_E(10 \text{ m}) = a_e + b_e u_{10}^{p_e} + c_e (u_{10} - 8)^2 \quad (7)$$

Numerical constants  $a_{h,e}$ ,  $b_{h,e}$ ,  $p_{h,e}$  and  $c_{h,e}$  vary with a range of wind speed as tabulated in Table 2. Relationship between  $q_a$  and  $e_a$  is also assumed as

$$q_a = 0.62 \frac{e_a}{P}, \quad (8)$$

$$e_a = 6.10781 \times 10^{-4} T_a^3 + 0.541493 T_a + 4.61967 \quad (9)$$

(Konda *et al.*, 1996).

The meanings of the variables and constants in the formulas are summarized in Table 3.

**Table 2.** Parameters in expressions for neutral bulk transfer coefficients.

$u_{10}$ (m s <sup>-1</sup> )	$a_h$	$a_e$	$b_h$	$b_e$	$c_h$	$c_e$	$p_h$	$p_e$
0.3 to 2.2	0	0	1.185	1.23	0	0	-0.157	-0.16
2.2 to 5	0.927	0.969	0.0546	0.0521	0	0	1	1
5 to 8	1.15	1.18	0.01	0.01	0	0	1	1
8 to 25	1.17	1.196	0.0075	0.008	-0.00045	-0.0004	1	1
25 to 50	1.652	1.68	-0.017	-0.016	0	0	1	1

**Table 3.** Values of the variables and constants in (2)~(5):  $I_0$  is referred to in Seckel and Beaudry (1973), Reed (1977).

Parameter	Symbol	Value and unit
Solar radiation under clear sky	$I_0$	W m <sup>-2</sup>
Albedo at the sea surface	$\alpha$	0.06
Emissivity at the sea surface	$\epsilon$	0.97
Stefan-Boltzmann constant	$\sigma$	$5.6705 \times 10^{-8}$ W m <sup>-2</sup>
Air temperature	$T_a$	K
Sea surface temperature	$T_s$	K
Vapor pressure	$e_a$	hPa
Saturation vapor pressure	$e_s$	hPa
Air density	$\rho$	1.225 kg m <sup>-3</sup>
Specific heat of air	$C_p$	1004.6 J kg <sup>-1</sup> m <sup>-3</sup>
Wind speed (10 m)	$U$	m s <sup>-1</sup>
Latent heat of evaporation	$L$	$2.50 \times 10^6$ J kg <sup>-1</sup>
Specific humidity	$q_a$	g kg <sup>-1</sup>
Saturated specific humidity at $T_s$	$q_s$	g kg <sup>-1</sup>

## 2.3 Turbulent kinetic energy and stability

Turbulent kinetic energy (TKE) which is a measure of the intensity of turbulence is one of the most important variables in micrometeorology, it is directly related to the momentum, heat and moisture transport through the boundary layer. TKE is also sometimes used as a starting point for approximations of turbulent diffusion.

The individual terms in the TKE budget equation describe physical processes that generate turbulence. The relative balance of these processes determines the ability of the flow to maintain turbulence or become turbulent, and thus indicates flow stability. Some important dimensionless groups and scaling parameters are also based on terms in the TKE equation.

The definition of TKE is  $\text{TKE}/m = \bar{e} = 0.5(\overline{u'^2} + \overline{v'^2} + \overline{w'^2})$ . TKE/m is nothing more than the summed velocity variances divided by two. Therefore, starting with the prognostic equation for the sum of velocity variances and dividing by two easily gives the TKE budget equation:

$$\begin{aligned}
 \frac{\partial \bar{e}}{\partial t} = & \underbrace{-\overline{u'w'}}_{\text{I}} \underbrace{\frac{\partial \bar{u}}{\partial z}}_{\text{II}} - \underbrace{\overline{v'w'}}_{\text{III}} \underbrace{\frac{\partial \bar{v}}{\partial z}}_{\text{IV}} - \underbrace{\frac{\partial (\overline{w'e'})}}_{\text{IV}} - \underbrace{\frac{1}{\rho} \frac{\partial (\overline{w'p'})}}_{\text{V}} \\
 & + \underbrace{\frac{g}{T} [(\overline{w'\theta'}) + 0.61T(\overline{w'q'})]}_{\text{VI}} - \underbrace{\epsilon}_{\text{VII}}.
 \end{aligned} \tag{10}$$

Term I represents local storage or tendency of TKE. Term II describes the advection of TKE by the mean wind. Term III is the buoyant production or consumption term. It is a production or loss term depending on whether the heat flux is positive or negative. Term IV is a mechanical or shear production/loss term. The momentum of the wind is usually lost downward to the ground. Thus, Term IV results in a positive contribution to TKE when multiplied by a negative sign. Term V represents the turbulent transport of TKE. Term VI is pressure correlation term that describes how TKE is redistributed by pressure perturbations. Term VII represents the viscous dissipation of TKE; i.e., the conversion of TKE into heat. Turbulence is dissipative. Term VII is a loss term that always exists whenever TKE is nonzero. Physically, this means that turbulence will tend to decrease and disappear with time, unless it can be generated locally or transported in by mean, turbulent, or pressure processes. Thus, TKE is not a conserved quantity (Stull, 1988).

Considering the wind direction along the average wind and neglecting relatively small terms,

$$-\overline{u'w'}\frac{\partial \bar{u}}{\partial z} + \frac{g}{T}[(\overline{w'\theta'}) + 0.61T(\overline{w'q'})] - \epsilon = 0. \quad (11)$$

In the surface layer where the flux is constant, we can substitute  $\overline{u'w'}$

for  $u_*^2$ . If the condition is close to neutral,

$$\frac{\partial \bar{u}}{\partial z} = \frac{u_*}{xz} \psi_m(z/L) \simeq \frac{u_*}{xz}, \quad (12)$$

$$-\frac{u_*^3}{xz} + \frac{g}{T} [(\overline{w'\theta'}) + 0.61 T(\overline{w'q'})] - \epsilon = 0. \quad (13)$$

Unstable flows become or remain turbulent. Stable flows become or remain laminar. There are many factors that can cause laminar flow to become turbulent, and other factors that tend to stabilize flows. If the net effect of all the destabilizing factors exceeds the net effect of the stabilizing factors, then turbulence will occur. In many cases, these factors can be interpreted as terms in the TKE budget equation.

To simplify the problem, investigators have historically paired one destabilizing factor with one stabilizing factor, and expressed these factors as a dimensionless ratio. Examples of these ratios are the Reynolds number, Richardson number, Rossby number, Froude number, and Rayleigh number.

Static stability is a measure of the capability for buoyant convection. The word "static" means "having no motion"; hence this type of stability does not depend on wind. The word "dynamic" refers to motion; hence, dynamic stability depends in part on the winds. Even if the air is statically stable, wind shears may be able to generate

turbulence dynamically. The static instability, combined with the continued dynamic instability, causes the flux to become turbulent.

The Obukhov length ( $L$ ) is a scaling parameter that is useful in the surface layer. To show how this parameter is related to the TKE equation, first recall that one definition of the surface layer is that region where turbulent fluxes vary by less than 10% of their magnitude with height. By making the constant flux (with height) approximation, one can use surface values of heat and momentum flux to define turbulence scales and nondimensionalize the TKE equation. In the TKE equation (10), the Obukhov length is defined by the ratio between the main turbulent production term ( $\Pi$  and  $\text{VI}$ ),

$$L = - \frac{u_*^3}{\kappa \frac{g}{T} \frac{H_0}{\rho C_p}} . \quad (14)$$

One physical interpretation of the Obukhov length is that it is proportional to the height above the surface at which buoyant factors first dominate over mechanical (shear) production of turbulence (Stull, 1988).

The parameter  $\zeta$  turns out to be very important for scaling and similarity arguments of the surface layer. It is sometimes called a stability parameter, although its magnitude is not directly related to static nor dynamic stability. Only its sign relates to static stability: negative



implies unstable, positive implies statically stable. A better description of  $\zeta$  is a surface-layer scaling parameter:

$$\zeta = z/L \text{ ,} \quad (15)$$

When the significant wave height ( $\sigma$ ) is considered as an important parameter in the surface layer, we can use

$$\zeta = \sigma/L. \quad (16)$$

### 3. Variations of the sea surface heat fluxes

#### 3.1 Monthly and annual means

The time variations of monthly mean values of  $Q_T$ ,  $Q_S$ ,  $Q_B$ ,  $Q_H$  and  $Q_E$  are shown in Fig. 2 over the Yellow Sea (YS) (Fig. 2(a)) and the South Sea (SS) (Fig. 2(b)). We use the convention, which a negative flux represents a transfer of heat from the ocean to the atmosphere. At the both sides,  $Q_S$  is the maximum in June and the minimum in December, ranges from about  $120 \text{ W m}^{-2}$  to  $340 \text{ W m}^{-2}$ . Variations of  $Q_S$  and  $Q_B$  show similar tendency since they are function of the latitude.

$Q_E$  is the most significant component for the heat exchange between air-sea over these regions except #22102, and usually much large in autumn and small in spring due to the difference of sea-air specific humidity (DQ) (Fig. 3).  $Q_E$  increases especially in autumn when the atmosphere is so dried. In the case of #22102 buoy, data is not enough.  $Q_E$  shows the negative value all through the year. This means that the large heat loss occurred from the sea surface. Over the YS,  $Q_E$  is the maximum as about  $200 \text{ W m}^{-2}$  in September and the minimum as about  $20 \text{ W m}^{-2}$  in June as mentioned in Na *et al.* (1999), but not in value. Over the SS, the maximum of  $Q_E$  is about  $280 \text{ W m}^{-2}$  in

September and the minimum about  $70 \text{ W m}^{-2}$  in May.

At the both sides,  $Q_H$  shows the positive value in spring and summer and the variation ranges within  $10 \text{ W m}^{-2}$ .  $Q_H$  also shows considerably the negative value in winter; the minimum about  $-80 \text{ W m}^{-2}$  in December over the YS and the minimum about  $-120 \text{ W m}^{-2}$  in February over the SS. In Fig. 1 and Fig. 2, it is noted that the variation of  $Q_E$  relies on the difference of the temperature between the air and the sea.  $Q_H$  decreases rapidly from October when the difference of sea-air temperature (DT) and wind speed (WS) are getting larger due to the influence of winter Asian monsoon, and becomes the minimum in December and January.

The maximum heat loss occurs in winter over the SS and the YS, as mentioned in Na *et al.* (1999).  $Q_T$  is the maximum in June as about  $290 \text{ W m}^{-2}$  and the minimum in December as about  $-190 \text{ W m}^{-2}$  over the YS, and is the maximum in May as about  $190 \text{ W m}^{-2}$  and the minimum in January as about  $-250 \text{ W m}^{-2}$  over the SS. This implies that the heat loss in winter is larger over the SS than over the YS. The annual mean variation of  $Q_T$  follows the pattern of  $Q_E$  in autumn and winter.

Large spatial differences between the YS and the SS are shown in Fig. 4. Like this, large spatial difference especially in winter is accounted mainly for the substantial DT, WS and DQ, which effect on

$Q_H$  and  $Q_E$ . In summer, the difference of  $Q_T$  between the YS and the SS is due to the DQ and the wind controlling  $Q_E$ . On a whole, the spatial difference of heat flux between the both sides appears evident. Considering the features of heat fluxes at the both sides, more heat loss is seen over the SS. Such an obvious spatial difference is basically caused by the effect of Tsushima Warm Current, and also equally seen from the results of Ishii *et al.* (1987) in which ten-year climatological data were compiled.

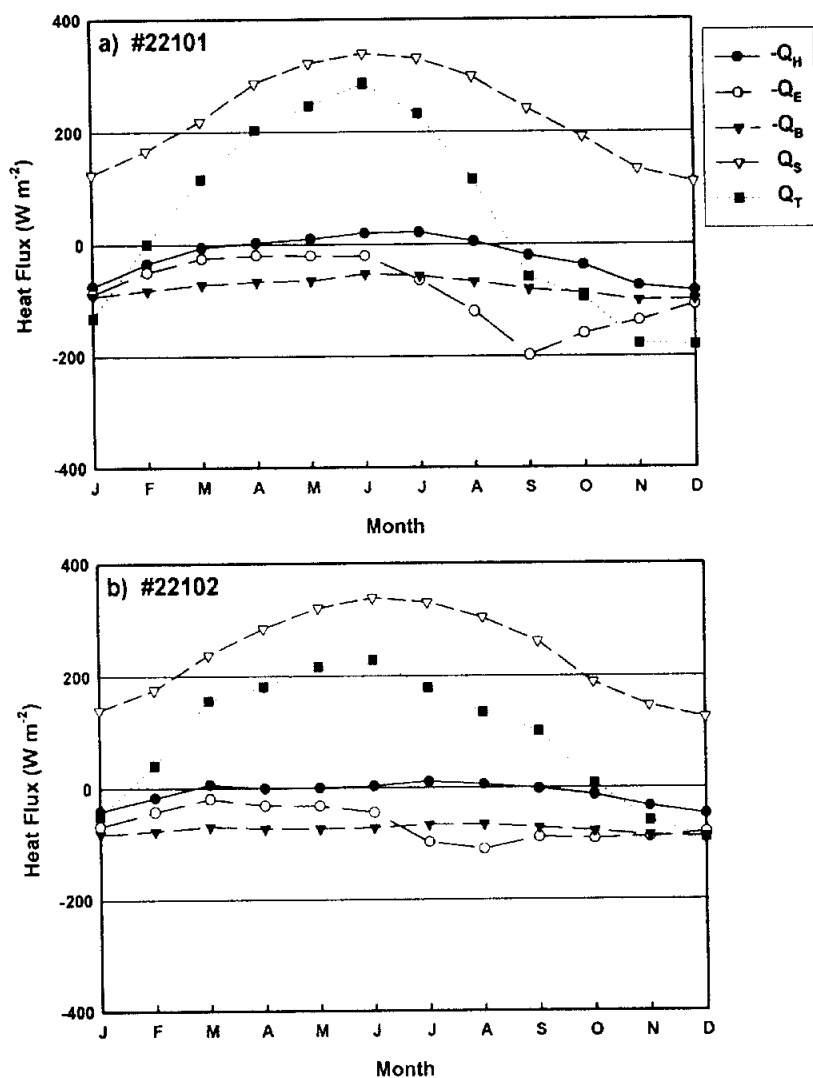


Fig. 2. The seasonal variation of the monthly mean fluxes over the Yellow Sea (#22101, #22102) and the South Sea (#22103, #22104) from 1996 to 2002.

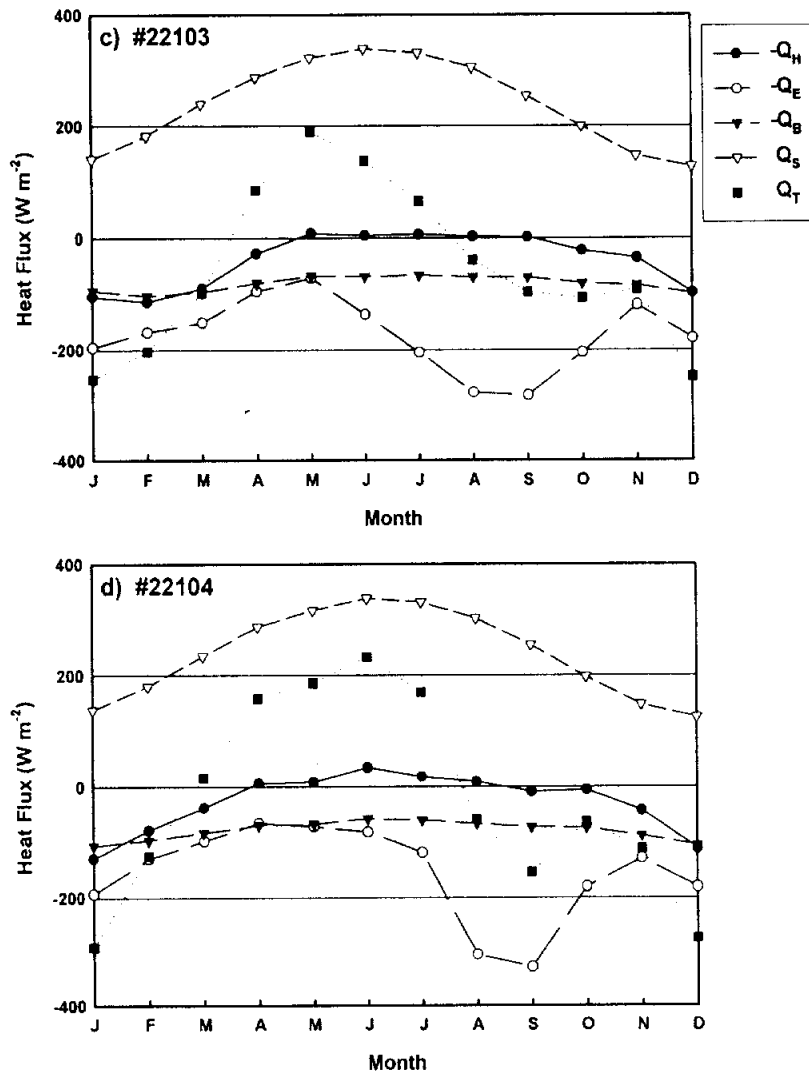
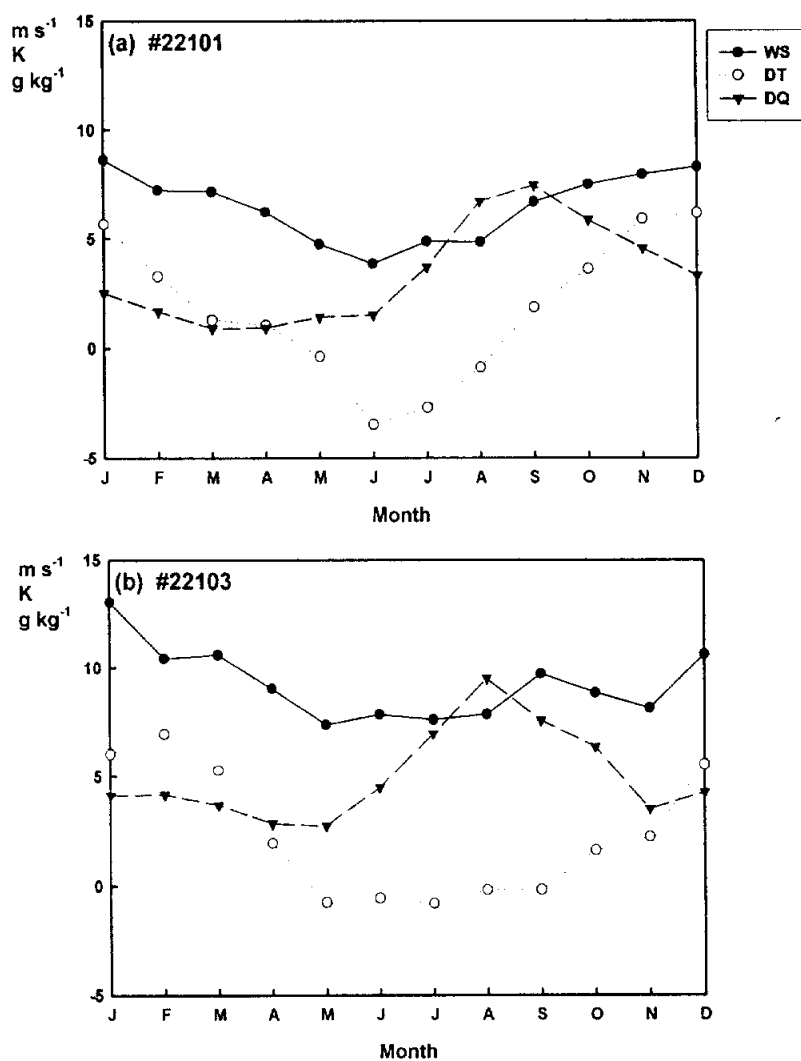


Fig. 2. continued.



**Fig. 3.** The seasonal variation of the monthly mean wind speed (WS), the difference of sea-air temperature (DT), the difference of sea-air specific humidity (DQ) over the Yellow Sea (#22101) and the South Sea (#22103) for the same period as Fig. 2.

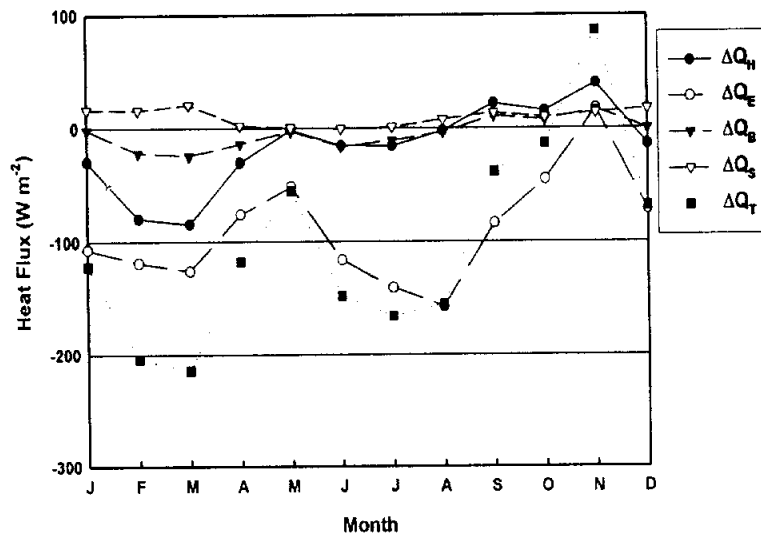


Fig. 4. The seasonal variation of the monthly mean spatial difference between the Yellow Sea (#22101) and the South Sea (#22103).



### 3.2 Diurnal means during winter season

Fig. 5 shows daily variations of meteorological parameters over the YS and the SS from December 2001 to February 2002 mainly situated from 1010 to 1030 hPa. The wind speed (WS) is relatively strong 8 m s<sup>-1</sup> or more (Fig. 5(b)). The variations of air temperature (AT) are analogous but not in magnitude at the both sides (Fig. 5(c)). AT varies about -8.5~4K and about 2~18K over the YS and the SS, respectively. The sea surface temperature (SST) over the YS decreases smoothly during this period, while SST over the SS according to meteorological conditions (Fig. 5(d)). A shallow sea might be influenced by wind forcing and coastal water (Na *et al.*, 1990). In Fig. 6, we analyzed the monthly wind directions for same period as Fig. 5 over the YS and the SS. They are mainly northwest winds, which is a general characteristic in the winter season. The variation of  $Q_T$  is much more remarkable over the SS and its amplitude over the SS is about 1.4 times as strong as over the YS (Fig. 7). This is attributed to the reason that  $Q_E$  accounting for a large portion of  $Q_T$  is much larger over the SS than over the YS (Fig. 8). The severe heat loss is also noticeable at the both sides on the second, 8th, and 22nd of January 2002. Kondo (1976) showed that a strong activities making an intensive interaction between the air-sea have occurred at the rate of about twice a month. As regards turbulent fluxes ( $Q_H$  and  $Q_E$ ) during this period (Fig. 8),  $Q_H$  varies

about  $20 \sim 350 \text{ W m}^{-2}$  at the both sides, except from 12th to 15th of January, which show negative heat flux due to the rise of AT caused by the snowfall.  $Q_E$  is strong over the SS than over the YS about  $10 \sim 200 \text{ W m}^{-2}$ . To explain difference of heat flux over the YS and the SS, we analyze the third period heat loss (from 21 to 24 Jan. 2002).

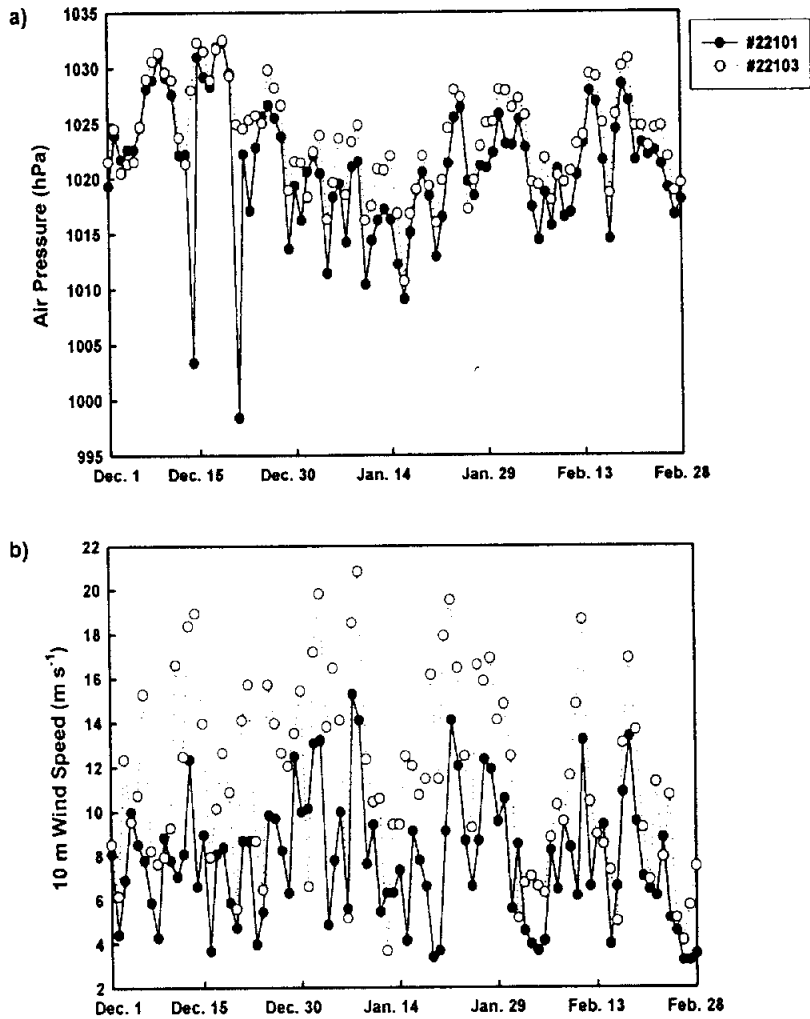


**Fig. 5.** Time series of the air pressure (P), wind speed (WS), air temperature (AT), and sea surface temperature (SST) over the Yellow Sea and the South Sea from December 2001 to February 2002.

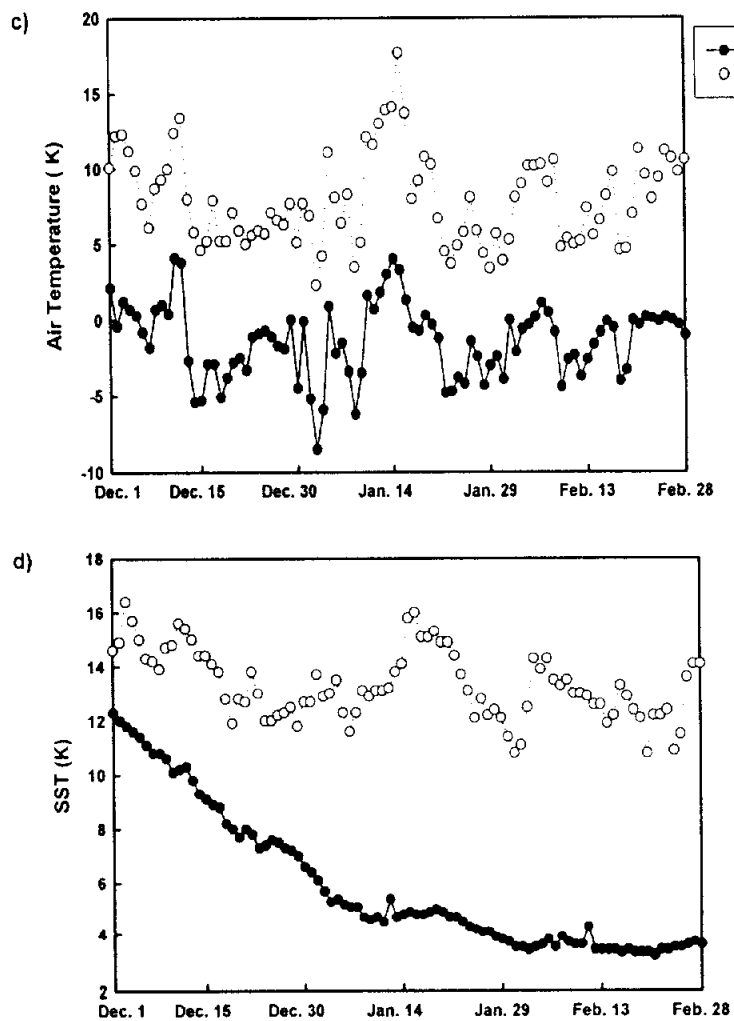


Fig. 5. continued.

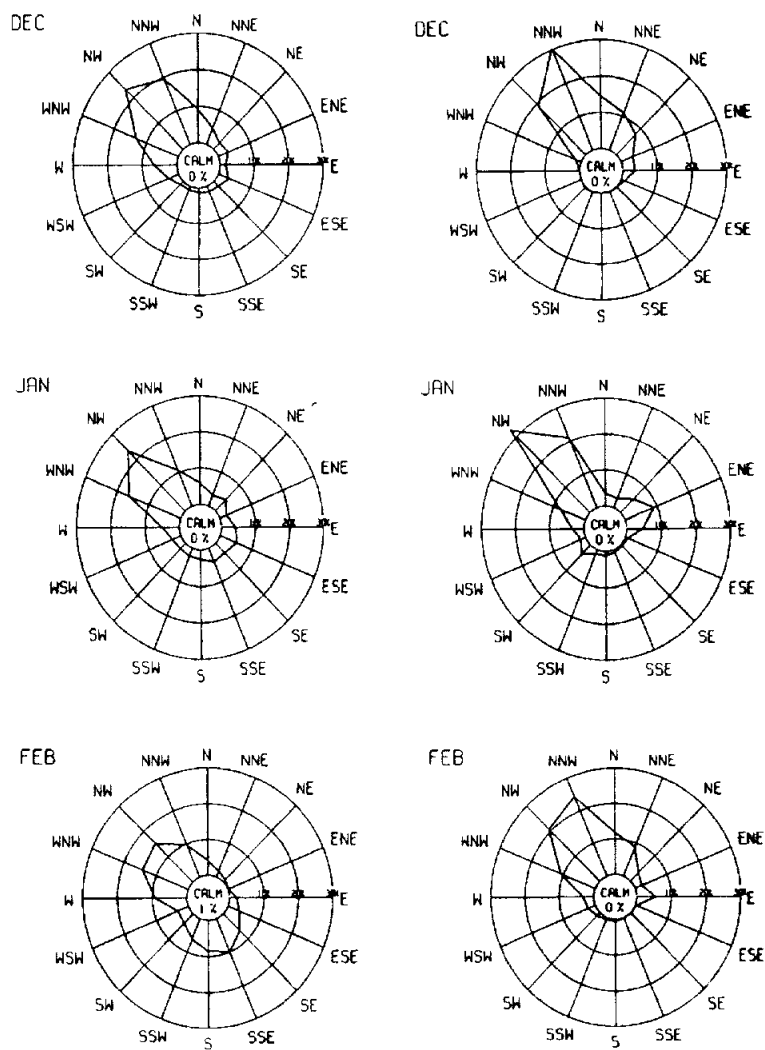
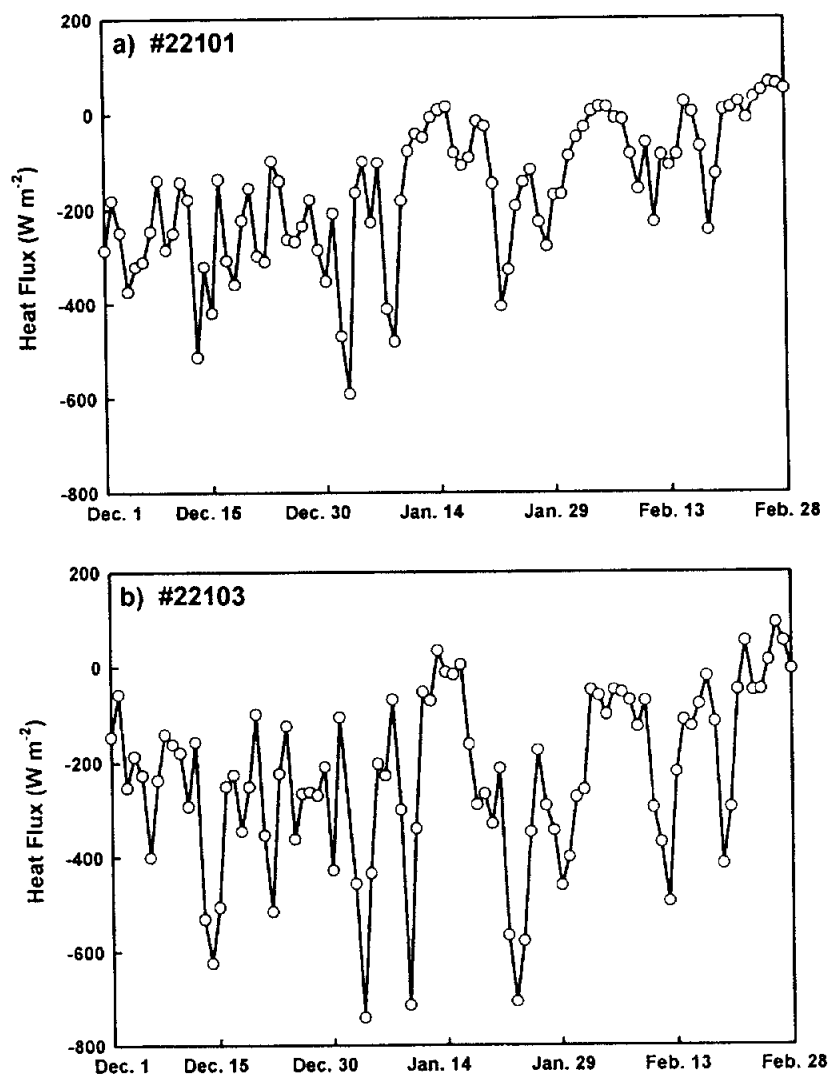
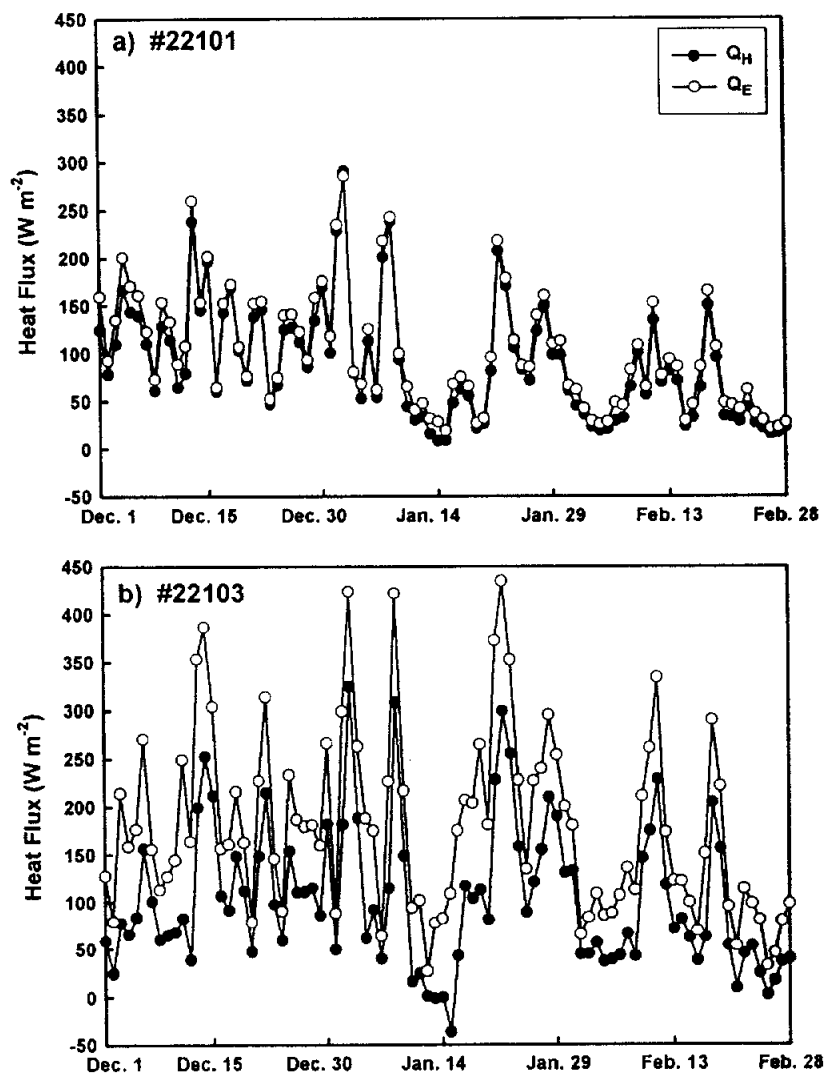


Fig. 6. Monthly wind roses over the Yellow Sea (left) and the South Sea (right) for the same period as Fig. 5.



**Fig. 7.** Time series of the total surface heat flux over (a) the Yellow Sea and (b) the South Sea for the same period as Fig. 5.



**Fig. 8.** Time series of the sensible heat ( $Q_H$ ) and latent heat ( $Q_E$ ) fluxes over (a) the Yellow Sea and (b) the South Sea for the same period as Fig. 5.

#### 4. Heat fluxes during the cold air outbreak

Fig. 9 shows the synoptic surface weather maps showing the cold air outbreak. A weak low pressure system over the east part of Siberia on 21~24, January 2002 moved over the East Sea where it began to intensify rapidly. A cold front, characterized by the strong cold air mass advection, also moved slowly. Due to the strong cold air mass advection, northwesterly winds and the rapid drop of air temperature were recorded at the buoys. Fig. 10 shows the time series of  $Q_H$  and  $Q_E$  during the typical cold air outbreak over the YS and the SS. Synoptic conditions play an important role in the dynamics near the sea surface. The values of  $Q_H$  and  $Q_E$  show a dramatic increase associated with approaching the cold front from the Asian continent to the warm ocean region. Such intensive air-sea interaction during the cold air outbreak can transform a continental air mass to one of maritime characteristics. This air mass transformation process represents a considerable input of energy from the sea into the air, a portion of which becomes available for the generation of storms (Agee *et al.*, 1977). The daily maximum heat loss during the cold air outbreak reaches up about  $-700 \text{ W m}^{-2}$  over the SS which is equivalent to three times as large as the averaged value in whole winter, and about  $-450 \text{ W m}^{-2}$  over the YS. Turbulent fluxes are similar pattern over the YS,  $Q_E$  over the SS is stronger than  $Q_H$ . Compared with the both sides,



$Q_H$  and  $Q_E$  are stronger over the SS than over the YS, which implies that the heat loss is larger over the SS than over the YS. In fact, the heat advection by the Kuroshio, which is out of phase with the shortwave radiation, decreases the amplitude of SST, while the heat advection by the Asian monsoon, which is out of phase with the shortwave radiation, increases the amplitude of SST (Kang, 1985). Time series of AT, WS and DQ ( $= q_s - q_a$ ) over the YS and the SS during this period are shown in Fig. 11. The variations of DT ( $= T_s - T_a$ ) are analogous at the both sides. It is well known that the DT in the open ocean is maximum in regions of the Kuroshio and the Gulf Stream where the heat advection is very large. The variations of WS and DQ are larger over the SS than over the YS. In general, the saturated vapor pressure is very low at the low temperature and increases exponentially with the temperature. DT is getting larger over the SS due to the increase of evaporation caused by high SST. In fact, the DT to control the sensible heat flux is analogous at the both sides (about  $7^\circ\text{C}$ ) and the DQ to control the latent heat flux is very large over the SS in the entire winter which corresponds to 1.4 times over the YS (Fig. 3).  $Q_H$  is larger due to WS over the SS than over the YS and  $Q_E$  is larger due to both WS and DQ over the SS than the YS.

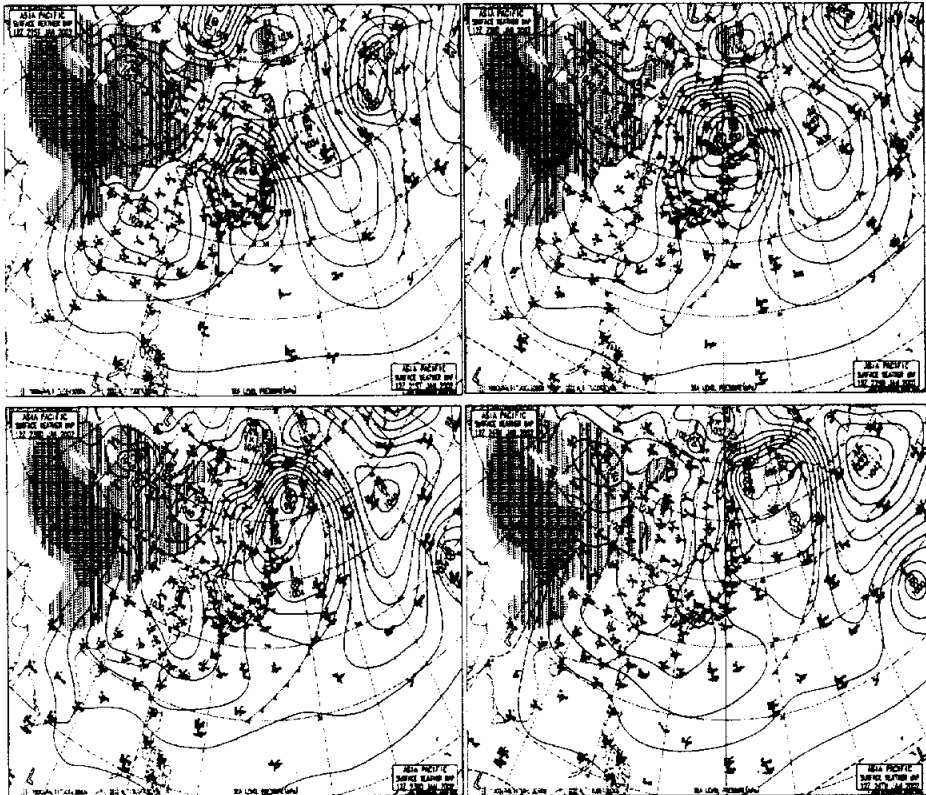


**Fig. 9.** Synoptic surface weather maps associated with the cold air outbreak from the 21st to 24th of January, 2002.

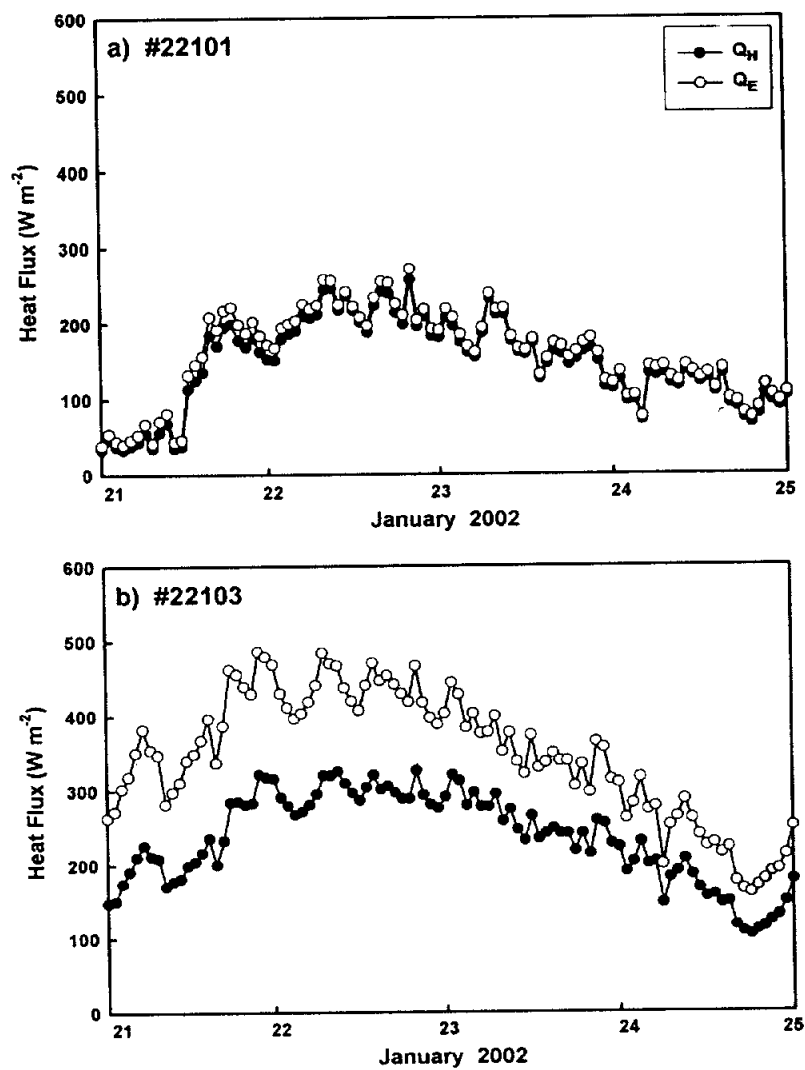


**Fig. 10.** Time series of the sensible heat ( $Q_H$ ) and latent heat ( $Q_E$ ) fluxes over (a) the Yellow Sea and (b) South Sea for the same period as Fig. 9.

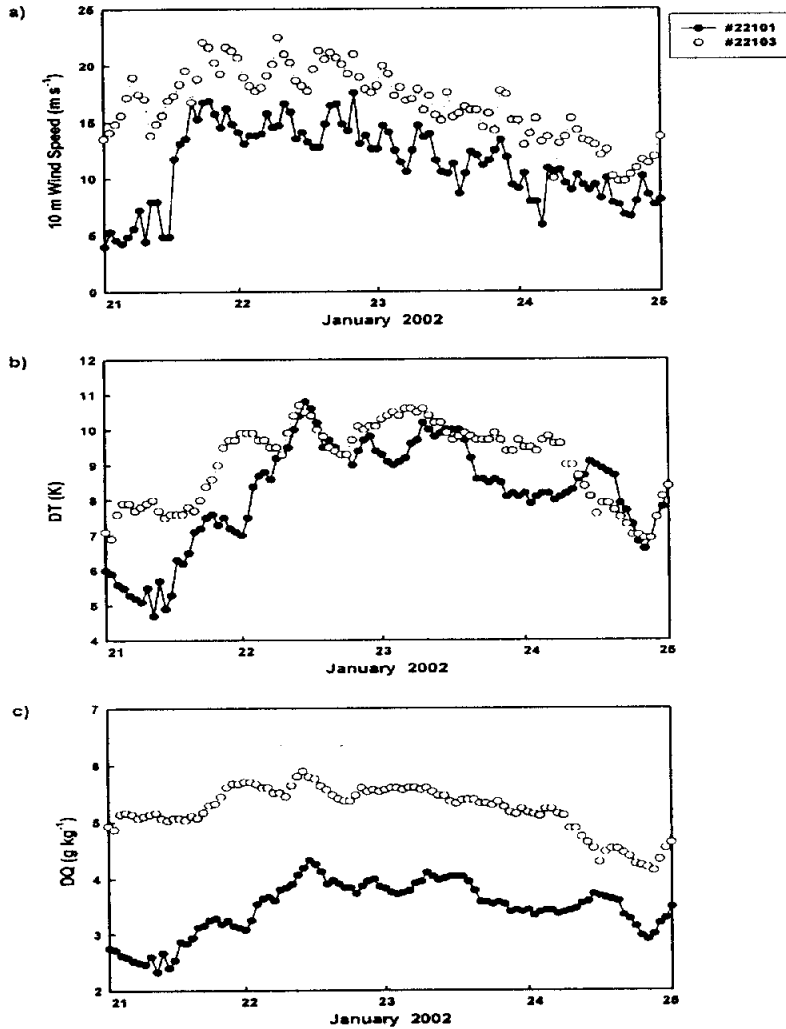


**Fig. 11.** Time series of the wind speed (WS), the difference of the sea-air temperature (DT), and the difference of sea-air specific humidity (DQ) over the Yellow Sea and the South Sea for the same period as Fig. 9.

## 5. Turbulent kinetic energy (TKE)

Turbulence refers to the apparently chaotic nature of many flows, which is manifested in the form of irregular, almost random fluctuations in velocity, temperature, and scalar concentrations around their mean values in time and space. The motions in the atmospheric boundary layer (ABL) are almost always turbulent. In the surface layer, turbulence is more or less continuous. Turbulence is responsible for the efficient mixing and exchange of mass, heat, and momentum throughout the ABL. In particular, the surface layer turbulence is responsible for exchanging these properties between the atmosphere and the sea surface. Without turbulence, such exchanges would have been at the molecular scale and minuscule in magnitudes. Mass exchange processes between the sea surface and the atmosphere, the radiation balance and the heat energy budget at or near the sea surface are also significantly affected. More direct effects of turbulent transfer on the surface heat energy budget are through sensible and latent heat exchanges between the sea surface and the atmosphere (Arya, 1988). The mechanism of  $Q_H$  and  $Q_E$  development can be analyzed from the viewpoint of a turbulent kinetic energy.

Fig. 12 shows comparisons of the dynamic energy production term and thermal energy production term between the YS and the SS from the TKE equation (11) during the winter season (Dec. 2001 ~ Feb. 2002).

Compared with the magnitude, the dynamic production is dominant at the YS (about 4 times as much as the thermal production) and at the SS (about  $10^2$  times). This means that the Marine Atmospheric Boundary Layer (MABL) is far from the convective boundary layer in winter at the both sides. The thermal production is about the same at the both sides and the dynamic production is more important over the SS than over the YS. Turbulence refer mainly to the wind which is a principal mechanism to transfer the heat from the both sides to the atmosphere. The surface layer become unstable by dynamic production during the cold air outbreak when the wind is stronger over the SS. It is noted that the production of TKE depends on the wind.

As an analysis of turbulent kinetic energy, Fig. 13 shows the stability parameter defined by the ratio between the dynamic production term and thermal production term. The atmosphere become unstable due to upward heat fluxes in winter. The stability parameter ( $\sigma/L$ ) with the significant wave height depending on the wind speed, shows comparable variation to  $z/L$ . Since the production of TKE is governed by dynamic term, the stability varies with the wind in the marine atmospheric surface layer. The range of instability is wide especially during the cold air outbreak over the YS and is not variable over the SS. A little variation of the stability implies that some properties of the atmospheric surface layer are conserved at that region. The fluctuation of SST over the SS (Fig. 5(d)) may maintain the TKE production ratio. Fig. 14

shows the distribution of friction velocities according to the stability during the cold air outbreak (from the 21st to 24th of Jan. 2002) and winter season (from Dec. 2001 to Feb. 2002) over the Yellow Sea and the South Sea are shown in Fig. 14. The friction velocity can characterize a great deal of the behavior of the atmospheric boundary layer, since the friction velocity reflects surface stress and is strongly modulated by surface buoyancy fluxes. It is found that the stability of the surface layer is closely associated to the wind speed during cold air outbreak and the intense wind results in an unstable surface layer. In Fig. 15, the stability is linked with the latent heat flux ( $Q_E$ ) during the cold air outbreak: the more it is getting unstable, the more  $Q_E$  increases during the cold air outbreak. Over the SS, the wide variation of  $Q_E$  despite a little variation of  $z/L$  means that  $Q_E$  depends on the difference of water vapor between the air and the sea than on the wind.

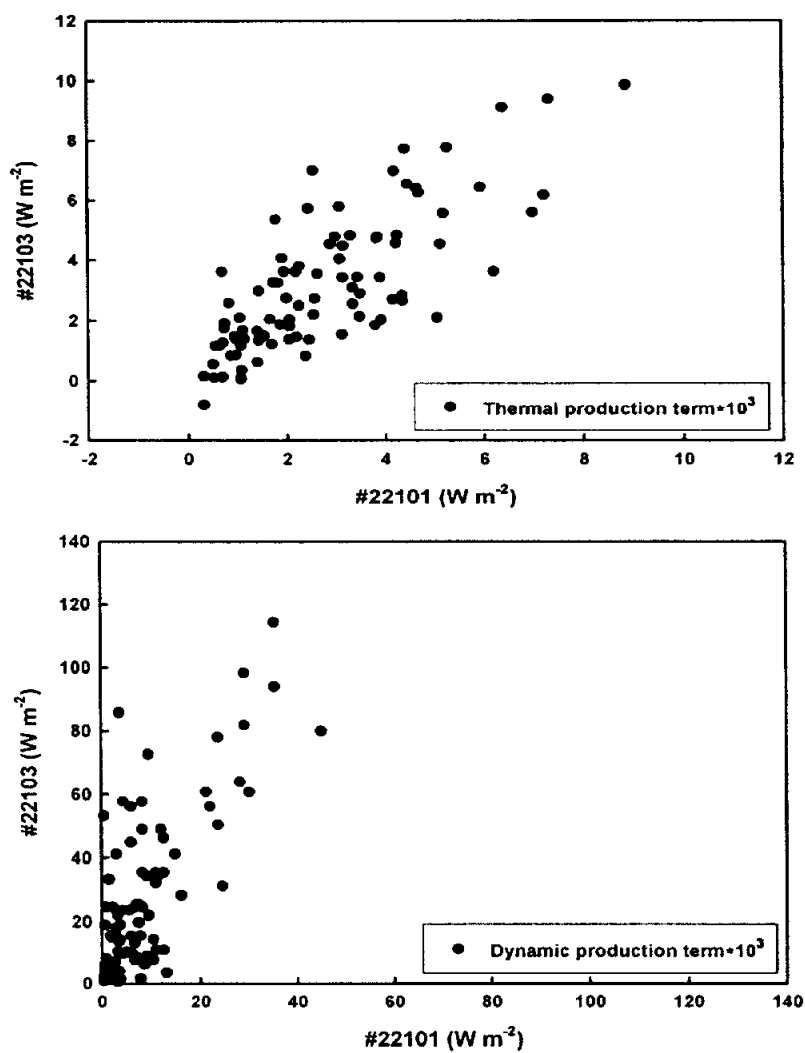
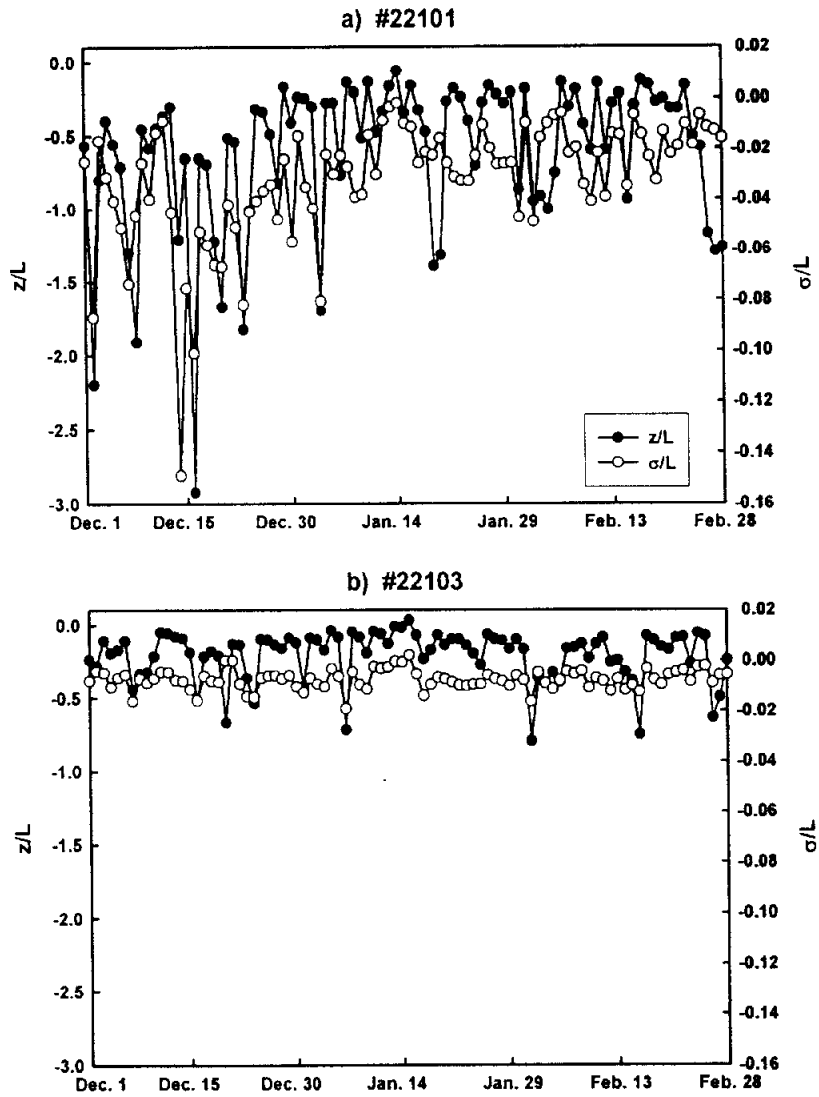


Fig. 12. Dynamic production term and thermal production term over the Yellow Sea (#22101) and the South Sea (#22103) from December 2001 to February 2002.





**Fig. 13.** Variation of the stability parameters ( $z/L$  and  $\sigma/L$ ) over the Yellow Sea (#22101) and the South Sea (#22103) for the same period as Fig. 12.

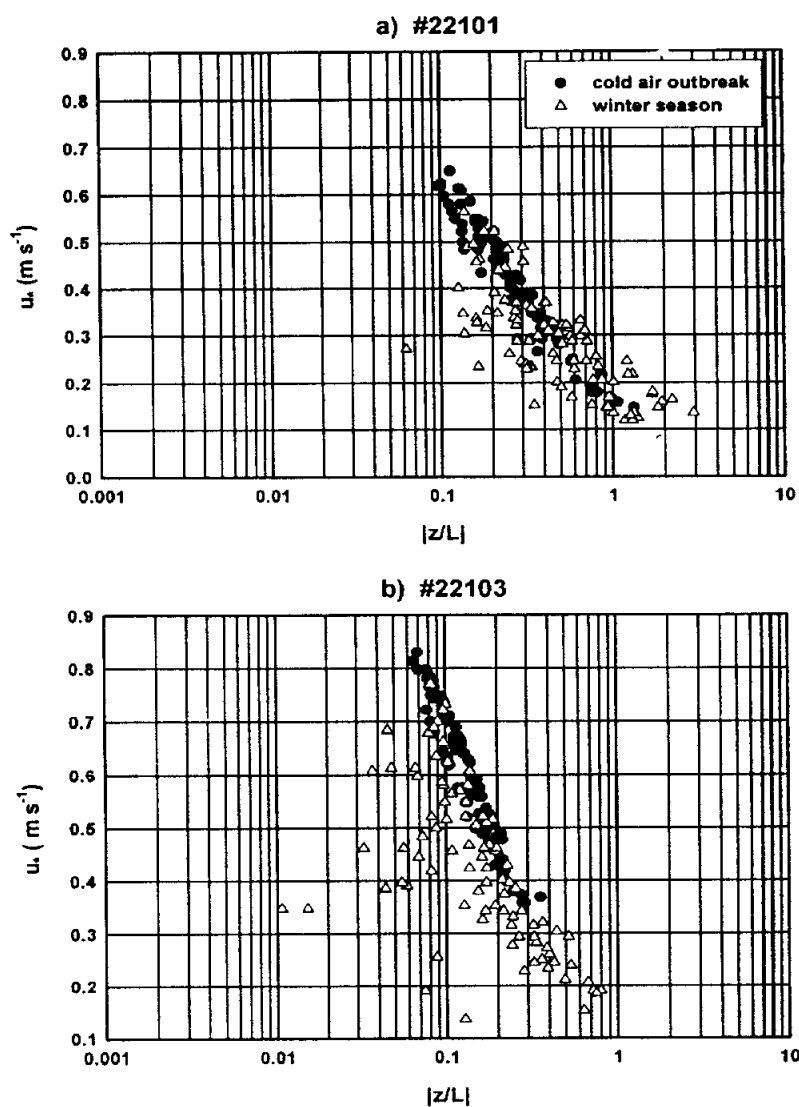


Fig. 14. Dependence of the friction velocity ( $u_*$ ) on the stability parameter  $z/L$  during the cold air outbreak and winter season over (a) the Yellow Sea and (b) the South Sea.

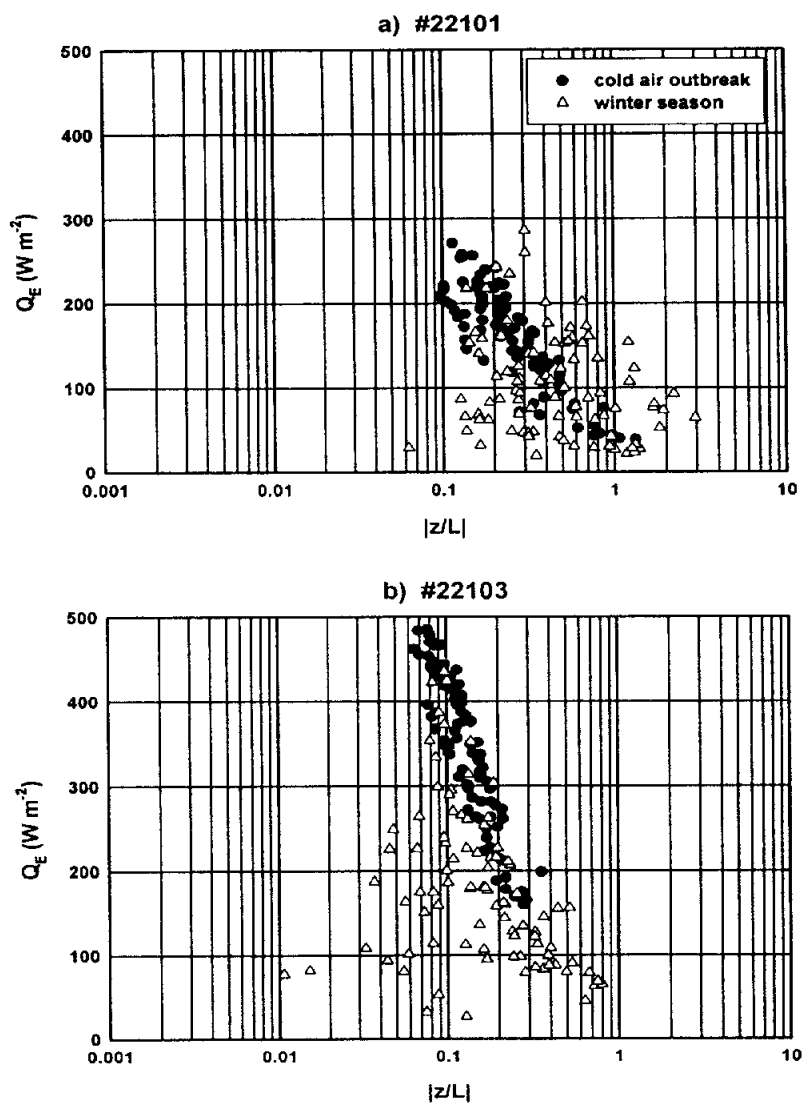


Fig. 15. Dependence of the latent heat flux ( $Q_E$ ) on the stability parameter  $z/L$  over (a) the Yellow Sea and (b) the South Sea for the same period as Fig. 14.

## 6. Conclusions

The heat fluxes are investigated based on the hourly ocean buoy data obtained over the Yellow Sea and the South Sea from July 1996 to May 2002.

The heat loss in winter is larger over the SS than over the YS. The annual mean variation of the total heat fluxes relies on rather the latent heat flux in autumn and winter.

At the both sides, the sensible heat flux increases rapidly from October due to the influence of winter Asian monsoon and becomes to maximum in December over the Yellow Sea, in January over the South Sea.

When an approach of intensive cold air mass front from Siberia to the Tsushima warm current region, the heat loss by the sensible heat and latent heat fluxes increases gradually.

The large sensible heat flux is accounted for intensity of wind and the large latent heat flux is related to both intensity of wind and difference of sea-air specific humidity over the South Sea.

During this period, turbulent parameters in the marine atmospheric surface layer over the sea show a clear increase with the stability. The friction velocity can characterize a great deal of the behavior of the atmospheric boundary layer, since the friction velocity reflects surface stress and is strongly modulated by surface buoyancy fluxes.

In the analysis of turbulent kinetic energy, the production of TKE is under the control of wind over the SS and the YS in winter. The stability of the surface layer depends on the wind speed during the winter season and is closely associated with the wind speed during the cold air outbreak. The instability over the SS varies little in winter, which implies that the marine atmospheric surface layer is well conserved.

## Reference

- Agee, E. M., and R. P. Howely, 1977: Latent and sensible heat flux calculation at the interface during AMTEX' 74. *J. Appl. Meteor.*, **16**, 443-447.
- Arya, S. P., 1988: *Introduction to Micrometeorology*. Academic Press, 307pp.
- Breaker, L. C., D. B. Gilhousen, and L. D. Burroughs, 1998: Preliminary results from long-term measurements of atmospheric moisture in the marine boundary layer in the Gulf of Mexico. *J. Atoms. Oceanic Technol.*, **15**, 661-676.
- Efimova, N. A., 1961: On methods of calculating monthly values of net longwave radiation (in Russian). *Meteor. Gidrol.*, **10**, 28-33.
- Geernaert, G. L. (ed.), 1999: *Air-Sea Exchange: Physics, Chemistry and Dynamics*. Kluwer Academic Publishers, 579pp.
- Han, Y. H., and S. D. Chang, 1978: Relation between the heat budget and the cold water in the Yellow Sea in winter. *Bull. Korean Fish. Tech. Soc.*, **14**, 1-14.
- Hirose, N., 1995: Heat budget in the neighboring seas around Japan. Master's Thesis, Kyushu Univ., 142pp.
- Hirose, N., C. H. Kim, and J. H. Yoon, 1996: Heat budget in the Japan Sea. *J. Oceanogr.*, **52**, 553-574.

- Hirose, N., H. C. Lee, and J. H. Yoon, 1999: Surface heat flux in the East China Sea and the Yellow Sea. *J. phys. Oceanogr.*, **29**, 401-417.
- Ichikawa, H., and R. C. Beardsley, 2002: The current system in the Yellow and East China Seas. *J. Oceanogr.*, **58**, 77-92.
- Ishii, T., and J. Kondo, 1987: Seasonal variation of the heat balance of the East China Sea. *Tenki*, **34**, 517-526.
- Joffre, S. M., M. Kangas, M. Heikinheimo, and S. A. Kitaigorodskii, 2001: Variability of the stable and unstable atmospheric boundary layer height and its scales over a boreal forest. *Boundary-Layer Meteor.*, **99**, 429-450.
- Kang, I. S., M. K. Kim, and T. B. Shim, 1994: Seasonal variation of surface heat budget and wind stress over the seas around Korean Peninsula. *J. Oceanol. Soc. Korea*, **29**, 325-337.
- Kang, Y.-J., S.-O. Hwang, T.-H. Kim, and J.-C. Nam, 2001: Estimation of air-sea heat exchange using buoy data at the Yellow Sea, Korea. *J. Korean Earth Sci. Soc.* **22**, 40-46.
- Kang, Y. Q., 1985: Influences of the Asian monsoon and the Kuroshio on the sea surfaces in the Yellow, the Japan and the East China Seas. *J. Oceanol. Soc. Korea*, **20**(2), 1-9.
- Kato, K., and T. Asai, 1983: Seasonal variations of heat budgets in both the atmosphere the sea in the Japan Sea area. *J. Meteor. Soc. Japan*, **61**, 222-238.

- Kim, M. K., and I. S. Kang, 1995: Diagnostic modeling of wind stress, sensible, and latent heat flux on the sea surface around the Korean Peninsula. *J. Korea Meteor. Soc.*, **31**, 1-13.
- Kim, Y. S., 1992: Estimate of heat transport across the sea surface near Japan with bulk methods. Doctoral Thesis, Univ. of Tokyo, 124pp.
- Kim, Y. S., and R. Kimura, 1995: Error evaluation of the bulk aerodynamic method for estimating heat flux over the sea. *J. Korean Meteor. Soc.*, **31**(4), 399-413.
- Kim, Y. S., and R. Kimura, 1999: Estimation of the heat flux exchanges between the air-sea Interface over the neighbouring seas of Korean Peninsula. *J. Korean Meteor. Soc.*, **35**, 501-510.
- Konda, M., N. Imasato, and A. Shibata, 1996: A new method to determine near sea surface air temperature by using satellite data. *J. geophys. research*, **101**, C6, 14349-14360.
- Kondo, J., 1975: Air-sea bulk transfer coefficients in diabatic condition. *Boundary-Layer Meteor.*, **9**, 91-112.
- Kondo, J., 1976: Heat balance of the East China Sea during the Air Mass Experiment. *J. Meteor. Soc. Japan*, **54**, 382-398.
- Kondo, M., 1985: Oceanographic investigations of fishing grounds in the East China Sea and the Yellow Sea- I , Characteristics of the mean temperature and salinity distributions measured at 50 m and near the bottom. *Bull. Seikai Region. Fish. Res. Lab.*, **62**, 19-55 (in Japanese with English abstract).



- Lie, H.-J., and C.-H. Cho, 1994: On the origin of the Tsushima Warm Current. *J. Geophys. Res.*, **99**, 25081-25091.
- Maizuru Marine Observatory (MMO), 1972: Marine meteorological study of the Japan Sea. *Tech. Rep. of the Japan Meteor. Agency*, **80**, 116pp. (in Japanese).
- Manabe, S., 1957: On the modification of air mass over East Sea when the outburst of air predominates. *J. Meteor. Soc. Japan*, **35**, 311-326.
- Manabe, S., 1958: On the estimation of energy exchange between the Japan Sea and the atmosphere during winter based upon the energy budget of both the atmosphere and the sea. *J. Meteor. Soc. Japan*, **36**, 123-134.
- Miyazaki, M., 1952: The heat budget in the Japan Sea. *Bull. Hokaido Reg. Fish. Res. Lab.*, **4**, 1-54.
- Na, J. Y., S. K. Han, and K. D. Cho, 1990: A study on sea water and ocean current in the sea adjacent to Korea Peninsula - Expansion of coastal waters and its effect on temperature variations in the South Sea of Korea. *Bull. Korean Fish. Soc.*, **23**, 267-279.
- Na, J. Y., J. W. Seo, and H. J. Lie, 1999: Annual and seasonal variations of the sea surface heat fluxes in the East Asian Marginal Seas. *J. Oceanogr.*, **55**, 257-270.
- Ninomiya, K., 1968: Heat and water budget over the Japan Sea and the Islands in winter season. *J. Meteor. Soc. Japan*, **46**, 343-372.

- Park, W. S., I. S. Oh, and T. B. Shim, 1995: Temporal and spatial distributions of heat fluxes in the East Sea (Sea of Japan). *J. Oceanol. Soc. Korea*, **30**, 91-115.
- Reed, R. K., 1977: On estimating insolation over the ocean. *J. Phys. Oceanogr.*, **7**, 482-485.
- Sakurai, M. A., A. Maeda and T. Yamasiro, 1989: The heat and water budget over the East China and the Yellow Seas. *Kaiyo Monthly, Symposium*, **21**, 412-415.
- Schlesinger, M. E. (ed.), 1990: *Climate-Ocean Interaction*. Kluwer Academic Publishers, 385pp.
- Seckle, G. R., and F. H. Beaudry, 1973: The radiation from sun and sky over the North Pacific Ocean (abstract). *Trans. Amer. Geophys. Union*, **54**, 114.
- Shim, T. B., and K. Kim, 1981: On the variation of the mixed layer depth and the heat flux in the Sea of Japan. *J. Oceanol. Soc. Korea*, **16**, 49-56.
- Stull, R. B., 1988: *An Introduction to Boundary Layer Meteorology*. Kluwer Academic Publishers, 666pp.
- Youn, Y.-H., S.-G. Hong, Y. Hong, and J. Y. Lee, 1998: A study on the estimation of air-sea heat fluxes and the wave characteristics using Chilbaldo buoy data. *J. Korea Soc. Ocean.*, **3**, 9-15.

## Acknowledgments

I would like to express my deepest appreciation to prof. Young-Ho Han, my advisor and mentor, for all of his advice, support and encouragement during the course of this thesis.

I am grateful to prof. Young-Seup Kim and prof. Byung-Hyuk Kwon for their helpful comments on this thesis and serving in my committee.

I would also like to thank prof. Dong-In Lee, prof. Hi-Ryong Byun, prof. Gon Ok, prof. Hyeong-Bin Cheong, and prof. Jai-Ho Oh for their valuable suggestions on this thesis.

I wish to thank to all members (Min-Jeong, So-Hee, Hyang-Mi, Jong-Min) of Atmospheric Remote Sensing Research Lab, for their kind assistance.

I would like to acknowledge my parents and sister (Mi-Ae) for their constant support and encouragement throughout my educational pursuit.

I wish to thank my friends (Tae Yarn, Liturtle, Hatz, Rane, Doyagi, and Kkang Mi, etc..) who have shared joys and sorrows with me.

Finally, I would like to thank everyone who have helped me in writing this thesis.